

## Third-harmonic generation in InAs/GaAs self-assembled quantum dots

S. Sauvage and P. Boucaud

*Institut d'Électronique Fondamentale, URA CNRS 22, Bâtiment 220, Université Paris-Sud, 91405 Orsay, France*

F. Glotin, R. Prazeres, and J.-M. Ortega

*CLIO/LURE, Bâtiment 209 D, Université Paris-Sud, 91405 Orsay, France*

A. Lemaître, J.-M. Gérard, and V. Thierry-Mieg

*Groupement Scientifique CNET-CNRS, 196 Avenue Henri Ravera, 92225 Bagneux, France*

(Received 1 December 1998)

We have observed third-harmonic generation associated with intraband transitions in semiconductor quantum dots. The frequency tripling ( $12\ \mu\text{m} \rightarrow 4\ \mu\text{m}$ ) occurs in the valence band of InAs/GaAs self-assembled quantum dots. We show that the third-harmonic generation is enhanced due to the achievement of the double resonance condition between intraband transitions. A third-order nonlinear susceptibility  $|\chi_{3\omega}^{(3)}|$  as large as  $1.5 \times 10^{-14}\ (\text{m/V})^2$  is measured for one dot plane. [S0163-1829(99)08211-9]

In two-dimensional (2D) semiconductor heterostructures, optical nonlinearities associated with intersubband transitions are known to be greatly enhanced as compared to nonlinearities in bulk semiconductors. Midinfrared second-<sup>1</sup> and third-harmonic<sup>2,3</sup> generation (THG) have been demonstrated in quantum wells along with other types of second- and third-order nonlinear processes.<sup>4</sup> Record third-order nonlinear susceptibilities, as large as five orders of magnitude greater than in bulk GaAs,<sup>2</sup> have been measured in coupled quantum wells. The enhancement of the nonlinearities in the quantum wells stems from the large oscillator strength of the intersubband transitions<sup>5</sup> and from the band-structure engineering, which enables us to satisfy the resonance conditions.

Large optical nonlinearities are also expected to occur in semiconductor quantum dots. The 3D confinement potential leads to a  $\delta$ -like density of states. The transitions between the confined levels in the conduction or in the valence band, referred to as intraband transitions in the following, have been observed using different techniques.<sup>6,7</sup> The optical nonlinearities associated with these intraband transitions are anticipated to be large for the following reasons. Like intersubband transitions in quantum wells, the intraband dipole lengths extend over the quantum dot size and are about a fraction of nm. The two- or three-photon resonance between excited states involved in the intraband transitions can also be achieved by choosing the dot size and geometry. In addition, the narrow homogeneous linewidth of the intraband transitions of individual quantum dots should contribute to

enhance the nonlinear susceptibility. Indeed, the intraband transitions are foreseen to be lifetime broadened as a direct consequence of the  $\delta$ -like density of states: any inelastic dephasing process corresponds to the scattering of the carriers from one level to another and is, therefore, associated with the lifetime of the carriers. Thus, by analogy with atomic physics, one expects for the quantum dots a direct correlation between the relaxation lifetime  $T_1$  and the coherence lifetime  $T_2$ , i.e.,  $T_2 = 2T_1$ . This feature is of importance since the quantum dot relaxation time is predicted to be slowed down due to the so-called “phonon bottleneck.”<sup>8</sup>

Based on these ideas, we have investigated the intraband optical nonlinearities in quantum dots. The standard self-assembled InAs/GaAs quantum-dot system grown by molecular beam epitaxy has been chosen and we have investigated the harmonic conversion in the midinfrared. We show in this paper that frequency tripling can be achieved in the valence band of the quantum dots. The resonant enhancement of the nonlinearity is demonstrated and a large third-order nonlinear susceptibility is deduced from our measurements, as a consequence of the large coherence lifetime, which is inherent to the quantum dots. Beyond this particular measurement, our results are of wide interest since they demonstrate that large intraband optical nonlinearities can be observed in three-dimensionally confined semiconductor heterostructures.

The nonlinear susceptibility involved in THG for a system close to triple resonance conditions is given by<sup>9</sup>

$$\chi_{3\omega}^{(3)} = \frac{e^4 N_{3D}}{\epsilon_0} \frac{\langle z_{01} \rangle \langle z_{12} \rangle \langle z_{23} \rangle \langle z_{03} \rangle}{(\hbar\omega - E_{01} - i\Gamma_{01})(2\hbar\omega - E_{02} - i\Gamma_{02})(3\hbar\omega - E_{03} - i\Gamma_{03})}, \quad (1)$$

where  $z_{ij}$  and  $\Gamma_{ij}$  are the dipole matrix elements and the broadening at half width at half maximum (HWHM) of the  $E_i - E_j$  transition, respectively,  $N_{3D}$  the 3D density of carriers,  $\epsilon_0$  the vacuum permittivity, and  $e$  the electronic

charge.<sup>10</sup> At given dipoles and carrier density, the maximum susceptibility is achieved in the triple-resonant case. In a previous paper,<sup>11</sup> we have shown that an intraband transition polarized along the growth axis direction is observed around

100 meV in the valence band and that the energy difference between the ground state and the wetting-layer continuum states is around 300 meV. Resonant THG for a  $\approx 12 \mu\text{m}$  pump wavelength appears, therefore, achievable in this system. The second key feature is that the transitions involved in the THG process need to have nonvanishing matrix elements. This condition is not fulfilled in the case of parabolic potential profiles ( $z_{03}=0$ ) but, as indicated by the calculations described below, achieved in the lens-shape quantum-dot geometry. Finally, we note that in the three-photon resonance conditions, the susceptibility is inversely proportional to the third power of the broadening.

The investigated quantum-dot structure consists of 40 InAs layers separated by 35-nm thick GaAs barriers. Details of the molecular beam epitaxy growth conditions can be found in Ref. 7. The dot density is around  $4 \times 10^{10} \text{cm}^{-2}$ . The quantum dots are modulation doped with a Beryllium  $\delta$ -doping layer located 2 nm above each InAs layer corresponding to a  $6 \times 10^{10} \text{cm}^{-2}$  bidimensional carrier density. Only the ground state of the quantum dots is thus populated. The quantum dot layers are inserted into a midinfrared waveguide in order to optimize the coupling of the midinfrared light to the  $z$ -polarized intraband transitions. The midinfrared waveguide consists of a 5.5- $\mu\text{m}$  thick GaAs core grown above a 5- $\mu\text{m}$  thick  $\text{Al}_{0.9}\text{Ga}_{0.1}\text{As}$  cladding layer. The quantum-dot layers are inserted in the middle of the GaAs core. The whole structure is grown on a  $n^+$ -doped ( $2 \times 10^{18} \text{cm}^{-3}$ ) GaAs substrate. The THG experiments have been performed at room temperature with a free-electron laser as a pump beam. The temporal profile of the free-electron laser consists of 10- $\mu\text{s}$  long macropulses at a repetition rate of 25 Hz. Each macropulse contains picosecond micropulses at a repetition rate of 31 MHz. The third-harmonic signal has been detected with a photovoltaic liquid-nitrogen-cooled InSb photodetector.

The energy levels and envelope wave functions of one InAs/GaAs quantum dot have been calculated by solving the 3D Schrödinger equation in the effective mass approximation.<sup>12</sup> The resolution is performed for a lens-shape quantum-dot geometry with an height around 3 nm and a base length around 25 nm, as observed by transmission electronic microscopy.<sup>13</sup> The effects of band bending are not taken into account by a self-consistent calculation since they will only lead to small corrections as compared to the quantum confinement energy. In the conduction band, the predicted energy levels are found in good agreement with those observed experimentally.<sup>11</sup> In the valence band, only the heavy-hole band has been considered and the InAs effective masses were decoupled between the  $z$  growth axis and the layer plane,  $m_z = 0.59 m_0$  and  $m_{x,y} = 0.07 m_0$  where  $m_0$  is the free-electron mass.<sup>11</sup> However, this simplified model leads to an overestimation of the calculated valence-band intraband transition energies. For simplicity and in order to reproduce the experimental intraband absorption spectrum, the height of the dot has been adjusted around 5 nm in the calculations, keeping constant the other parameters. Figure 1 depicts the calculated valence-band energy structure of one InAs/GaAs quantum dot. The levels involved in the  $z$ -polarized intraband transitions are marked in bold. In a parallelepipedal quantum dot with infinite potential barriers where confined states  $h_{n_x, n_y, n_z}$  can be sorted according to the number of

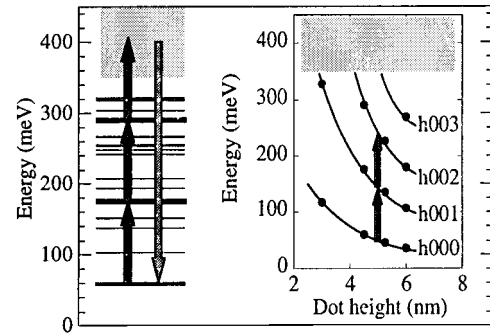


FIG. 1. First 19 calculated valence-band states of a InAs/GaAs quantum dot (4.5 nm height, 25 nm base diameter). The  $h_{000}$ ,  $h_{001}$ , and  $h_{002}$  states participating to the third-harmonic process are marked in bold. The THG is schematically depicted by the arrows. The gray zone corresponds to the wetting layer states. The inset shows the energy dependence of the  $h_{000}$ ,  $h_{001}$ ,  $h_{002}$ , and  $h_{003}$  levels vs the dot height for a fixed aspect ratio. The double arrows correspond to the dot size for which the  $h_{000}-h_{001}$  and  $h_{001}-h_{002}$  intraband energies are equal.

nodes  $n_x, n_y, n_z$  along the  $x, y$ , and  $z$  directions, these states would correspond to the  $h_{000}$ ,  $h_{001}$ , and  $h_{002}$  levels. The  $h_{003}$  level is confined for dots with a height larger than 5.5 nm and is hybridized with the wetting-layer states for smaller sizes. For a 5 nm height quantum dot, the dipole matrix elements  $z_{01}$  and  $z_{12}$ , which correspond to the  $h_{000}-h_{001}$  and  $h_{001}-h_{002}$  intraband transitions are 0.4 and 0.8 nm, respectively. Note that the  $z_{02}$  dipole-matrix element associated with the  $h_{000}-h_{002}$  intraband transition is almost zero ( $z_{02} = 4 \times 10^{-4} \text{nm}$ ). The energy dependence of the preceding levels vs the quantum-dot height is presented in the inset of Fig. 1. The energies of the intraband transitions vary as a function of the dot size as a consequence of the change in the confining volume. A careful analysis of the data shows that the double-resonance condition ( $h_{000}-h_{001}$  transition energy equals  $h_{001}-h_{002}$  transition energy) is achieved for a narrow dot size distribution with a 5-nm height.

The linear midinfrared absorption spectrum of the  $p$ -doped sample is reported in Fig. 2. The spectrum has been recorded for a 5-mm long sample in the TM polarization (polarization along the growth axis of the dots). The transmission has been normalized with the transmission spectrum of a reference waveguide containing undoped quantum-dot layers. The  $h_{000}-h_{001}$  transition is clearly observed at around 110 meV with an inhomogeneous broadening

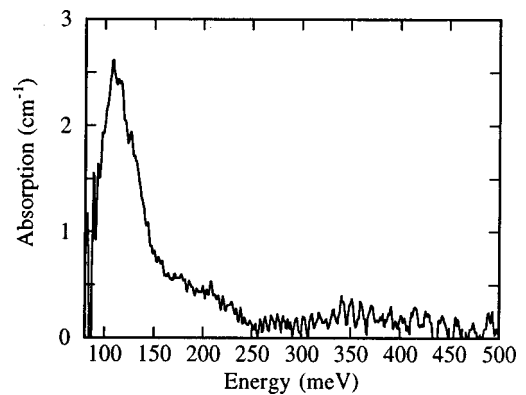


FIG. 2. Room temperature midinfrared linear absorption spectrum ( $h_{000}-h_{001}$  transition) of the  $p$ -doped InAs/GaAs self-assembled quantum dots.

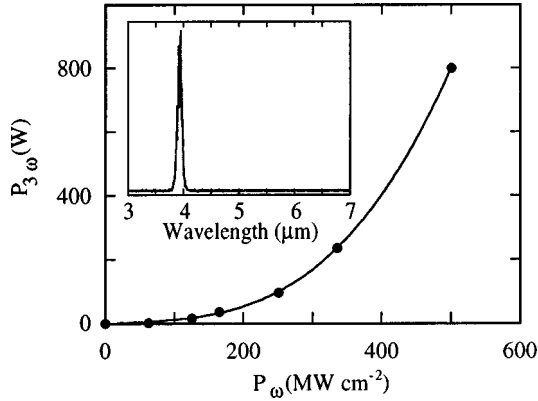


FIG. 3. Third-harmonic power ( $W$ ) vs the pump intensity ( $W\text{ cm}^{-2}$ ). The pump wavelength is set at  $11.9\ \mu\text{m}$  and focused on a  $300\ \mu\text{m}$  diameter spot. The full curve is a simulation according to Eq. (2). The spectrum of the generated third-harmonic signal is depicted in the inset.

(HWHM)  $\approx 18\text{ meV}$ . According to the simulations reported in Fig. 1, the present intraband absorption corresponds to a dot size distribution with an average height of  $4.7\text{ nm}$  and a size fluctuation of  $\pm 12\%$ . From the absorption amplitude, one can deduce the matrix element  $z_{01} \approx 0.35\text{ nm}$ , which is in agreement with the theoretical value ( $0.4\text{ nm}$  for a  $5\text{ nm}$  height quantum dot). A weak absorption above  $300\text{ meV}$  is also observed, which corresponds to the transition from the ground state to the continuum states lying above the wetting layer.

Relaxation time measurements have been performed on this sample with the free-electron laser by saturation spectroscopy of the  $h_{000}-h_{001}$  transition along with time-resolved measurements. Both experiments indicate that the relaxation time  $T_1$  associated with the  $h_{001}$  excited level is of the order of  $1.5\text{ ps}$ .<sup>14</sup> We suppose that this relaxation time corresponds to the lifetime of the excited level. Assuming  $T_2 = 2T_1$ , the linewidth (HWHM) of the  $h_{000}-h_{001}$  intraband transition is, therefore, estimated around  $200\ \mu\text{eV}$  for an individual quantum dot.

The third-harmonic power vs the pump intensity is presented in Fig. 3. The pump wavelength is  $11.9\ \mu\text{m}$ . The inset shows the spectrum of the detected signal, which is maximum at  $3.96\ \mu\text{m}$ . The third-harmonic signal is, as expected, proportional to the cube of the pump intensity. The third-harmonic power is TM polarized and is maximum when the pump is set in TM polarization. When the pump polarization is rotated by an angle  $\Phi$  from the TM direction, the third-harmonic signal decreases following the expected  $\cos^6 \Phi$  law associated with the polarization of the intraband absorption. This polarization dependence indicates that the intraband transitions involved in the third-harmonic process are polarized along the  $z$ -growth axis. The absence of THG in TE polarization rules out the possibility that the signal stems from the GaAs bulk material. This assumption is also confirmed by the fact that we did not observe THG in the same waveguide structure with  $n$ -doped quantum dots. The nonlinear process is thus clearly attributed to the intraband transitions in the quantum dots. Note that we did not observe second-harmonic generation in the present configuration. This is in agreement with the theoretical calculations, which predict that the dipole-matrix element  $z_{02}$  is nearly equal to

zero. It also excludes a two-step process by sum-frequency generation between the second harmonic and the fundamental beams.

The question now arises as to whether phase matching is achieved in the waveguide. In bulk GaAs, phase matching does not occur and the index difference between the pump and tripled signal leads to a coherence length  $\approx 50\ \mu\text{m}$ . The waveguide used in the present experiments is single mode at  $11.9\ \mu\text{m}$ , but multimode at  $3.9\ \mu\text{m}$ . One could envisage that phase matching occurs with a high-order mode with an effective index satisfying the condition  $n_{3\omega} = n_{\omega}$  as reported in Ref. 3. However, the waveguide mode calculations clearly show that the smallest effective index difference  $n_{3\omega} - n_{\omega}$  observed between the fundamental mode at  $\omega$  and the second excited mode at  $3\omega$  remains of the order of  $3 \cdot 10^{-2}$  close to the difference in the bulk material, thus excluding the occurrence of phase matching. From the calculated index difference vs pump wavelength, it appears that the third-harmonic conversion typically occurs over a  $50\ \mu\text{m}$  effective length.<sup>15</sup> The third-harmonic power is given by Eq. (2),<sup>2</sup> which in turn allows us to estimate the nonlinear susceptibility from the results presented in Fig. 3:

$$P_{3\omega} = \frac{3\mu_0^2 \omega^2 L^2 |\chi_{3\omega}^{(3)}|^2 P_{\omega}^3}{4n_{\omega}^3 n_{3\omega} S^2}, \quad (2)$$

where  $\mu_0$  is the vacuum permittivity,  $\omega$  the pump pulsation,  $n_{\omega}$  and  $n_{3\omega}$  the refractive indexes for the pump and third harmonic,  $L$  the interaction length,  $|\chi_{3\omega}^{(3)}|$  the third-order nonlinear susceptibility,  $S$  the area of the pump beam, and  $P_{\omega}$  the pump power coupled in the waveguide. Starting from Eq. (2), one finds  $|\chi_{3\omega}^{(3)}| \approx 9.5 \times 10^{-17}\text{ (m/V)}^2$ . The preceding value of susceptibility is an average value over the 40 dot planes embedded in the waveguide. Assuming a 0.6% overlap factor of the dot planes with the  $11.9\ \mu\text{m}$  pump beam,<sup>16</sup> one finds  $|\chi_{3\omega}^{(3)}| \approx 1.5 \times 10^{-14}\text{ (m/V)}^2$  for one dot layer plane. This value is of the same order of magnitude than the highest value of nonlinear susceptibility around  $10.7\ \mu\text{m}$  wavelength reported in  $\text{In}_x\text{Ga}_{1-x}\text{As}/\text{Al}_x\text{In}_{1-x}\text{As}$  quantum wells:  $|\chi_{3\omega}^{(3)}| \approx 10^{-14}\text{ (m/V)}^2$ . Although the matrix elements of the transitions are smaller for the quantum dots than for the quantum wells, the reduced homogeneous linewidth of the intraband transitions, which is an inherent property of the quantum dots, significantly enhances the nonlinear susceptibility. It is worth noticing that the use of quantum dots with a higher areal density and a better homogeneity should lead to much higher values of susceptibilities.

The theoretical nonlinear susceptibility can be directly calculated from Eq. (1). The number of dots excited by the picosecond pulse is given by the ratio of the pump spectral width and the inhomogeneous broadening of the  $h_{000}-h_{001}$  transition (3%). Since only the ground state is populated, only the transitions starting from the ground hole state are considered. In order to theoretically evaluate the nonlinear susceptibility, we will consider an ideal case in which: (i) the triple-resonance condition is achieved; (ii) the four states involved in the third-harmonic process are confined in the dot; (iii) the homogeneous linewidth corresponding to the three denominator terms in Eq. (1) are equal to  $200\ \mu\text{eV}$ . Using the calculated dipole matrix elements for a 6-nm height quantum dot for which the  $h_{003}$  level is bound ( $z_{01}$

$= 0.47$  nm,  $z_{12} = 0.83$  nm,  $z_{23} = 1.01$  nm, and  $z_{03} = 0.042$  nm), the peak nonlinear susceptibility is found as high as  $1.3 \times 10^{-12}$  (m/V)<sup>2</sup>. Experimentally, the  $h_{003}$  state is hybridized with the wetting layer states. We interpret the discrepancy between the experimental nonlinear susceptibility and the ideal theoretical nonlinear susceptibility mainly as a consequence of the hybridization of the  $h_{003}$  state. A rigorous calculation of the nonlinear susceptibility involving an hybridized state would require to integrate the susceptibility given by Eq. (1) over the states of the continuum in close resonance with  $3\hbar\omega$ . The susceptibility resulting of this integration should take into account the dipoles of the numerous transitions towards such states and the homogeneous linewidth of these transitions. However, in a simplified view, one will note that the difference between the experimental nonlinear susceptibility and the ideal theoretical one can be accounted for by a 17 meV detuning for the three-photon resonance, all other parameters (double resonance, homogeneous broadening, dipole-matrix elements) being kept constant. It is reassuring that this detuning is very close to the 15 meV detuning for the three-photon resonance ( $3\hbar\omega - E_{03}$  with  $\hbar\omega \approx E_{12}$ ), which is calculated when the  $h_{003}$  state is bound.

The nonlinear susceptibility deduced from the third-harmonic power dependence vs the pump energy is reported in Fig. 4. The third-harmonic process is strongly resonant with a maximum at 103 meV and a 4 meV full width at half maximum. The maximum conversion is achieved at an energy that is 7 meV below the absorption maximum. The narrow linewidth, which is much lower than the  $h_{000} - h_{001}$  absorption linewidth (36 meV), clearly indicates that a resonance condition is achieved for a narrow distribution of dot size. This is in agreement with the theoretical results reported in Fig. 1, which show that the *double resonance* condition can only be fulfilled for a small fraction of quantum dots. The dependence of the nonlinear susceptibility vs the photon energy has been computed starting from Eq. (1) and the energy dependence of the confined levels ( $h_{000}, h_{001}, h_{002}$ ) with the dot size. We have assumed a constant 17 meV detuning for the three-photon resonance. The nonlinear susceptibility is integrated over the inhomoge-

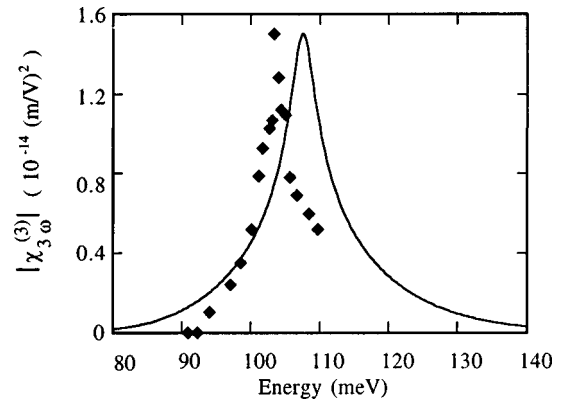


FIG. 4. Experimental nonlinear susceptibility  $|\chi_{3\omega}^{(3)}|$  (diamonds) vs the pump photon energy. The full line is a theoretical estimate of the susceptibility based on Eq. (1) and the calculated dependence of the energy levels as a function of the dot size.

neous size distribution of the dots. The result is reported as a full line in Fig. 4. The calculations predict an enhancement of the nonlinear susceptibility when the double resonance condition is achieved. The maximum of the susceptibility occurs at 107 meV, close to the 103 meV experimental value, with a 8 meV broadening. The calculated width of the resonance is a direct consequence of the energy level variation with the dot size. The larger theoretical broadening (8 instead of 4 meV) indicates that the variations of intraband energies vs quantum dot size are more pronounced than the calculated ones.

In conclusion, we have investigated intraband harmonic conversion in InAs/GaAs self-assembled quantum dots. We have shown that the choice of valence-band intraband transitions can satisfy the requirements for resonant THG. The nonlinear susceptibility has been found to be enhanced by the  $\delta$ -like density of states of the dots. A value of  $|\chi_{3\omega}^{(3)}| \approx 1.5 \times 10^{-14}$  (m/V)<sup>2</sup> has been deduced for one dot layer, which demonstrates that intraband nonlinearities in semiconductor quantum dots can be extremely large in the midinfrared.

This paper was partly supported by DGA under Contract No. 97062/DSP.

<sup>1</sup>M. M. Fejer *et al.*, Phys. Rev. Lett. **62**, 1041 (1989).

<sup>2</sup>C. Sirtori *et al.*, Phys. Rev. Lett. **68**, 1010 (1992).

<sup>3</sup>J. N. Heyman *et al.*, Phys. Rev. Lett. **72**, 2183 (1994).

<sup>4</sup>E. Rosencher *et al.*, Science **271**, 168 (1996).

<sup>5</sup>L. C. West *et al.*, Appl. Phys. Lett. **46**, 1156 (1985).

<sup>6</sup>H. Drexler *et al.*, Phys. Rev. Lett. **73**, 2252 (1994).

<sup>7</sup>S. Sauvage *et al.*, Appl. Phys. Lett. **71**, 2785 (1997).

<sup>8</sup>H. Benisty *et al.*, Phys. Rev. B **44**, 10 945 (1991).

<sup>9</sup>Y. R. Shen, *The Principles of Nonlinear Optics* (Wiley, New York, 1984).

<sup>10</sup> $z$ -polarized or in-plane polarized intraband transitions can be involved in nonlinear processes. Above 90 meV, we have mainly observed  $z$ -polarized intraband transitions and the THG involves only  $z$ -polarized transitions, hence the notation  $z_{ij}$  for the dipole matrix elements.

<sup>11</sup>S. Sauvage *et al.*, Phys. Rev. B **58**, 10 562 (1998).

<sup>12</sup>M. Grundmann *et al.*, Phys. Rev. B **52**, 11 969 (1995).

<sup>13</sup>J. M. Gérard *et al.*, Solid-State Electron. **40**, 807 (1996).

<sup>14</sup>This time duration is surprisingly short if it is compared to the times predicted by the slowing of the relaxation in the quantum dots. Note that the values of hole intradot relaxation time reported in the literature vary from 0.6 ps [T. S. Sosnowski *et al.*, Phys. Rev. B **57**, R9423 (1998)] to 40 ps [R. Heitz *et al.*, *ibid.* **57**, 9050 (1998)]. Note that the 1.5 ps hole relaxation time reported in this paper is measured at room temperature under high pump intensity. See S. Sauvage *et al.*, Appl. Phys. Lett. **73**, 3818 (1998).

<sup>15</sup>The harmonic conversion exhibits an oscillatory behavior as a function of the pump wavelength. The collected signal is therefore averaged over the spectral width of the picosecond pulse.

<sup>16</sup>The susceptibility is calculated with a 3D density of carriers for comparison purposes with other materials. The conversion between 2D and 3D carrier density involves the deposited InAs effective thickness ( $\approx 2$  ml), which appears in the confinement factor.